PREDICTION OF SMOKE VISIBILITY DURING AN UNDERGROUND RAIL STATION FIRE

K. Kang
Jacobs Inc., 260 Madison Avenue, New York, NY 10016, USA

ABSTRACT

Among all the tenability criteria, reduction in visibility due to smoke obscuration has been regarded as the most critical factor in fire life safety. This is especially important for smoke management in underground spaces such as rail stations. This paper presents an approach to predict visibility from CFD and quantifies smoke visibility as a line integral using a simplified ray-tracing model. The application of this model is demonstrated for a mid-platform train fire scenario in an underground rail station. Both natural ventilation and a concept of mechanical ventilation are studied, and the visibility conditions are compared at three selected locations along the egress paths. Quantitatively, the smoke layer height on the platform and the change of visibility on the mezzanine are evaluated, from which a better understanding is obtained on the effectiveness of the emergency ventilation. The egress accessibility during emergency evacuation and further developments of the smoke visibility model are discussed.

KEYWORDS: Visibility, Smoke control, Underground rail station, CFD

INTRODUCTION

Effective smoke control is important during an underground rail station fire. Given the tragic fire incidents in the Daegu city subway in Korea (2003) [1], the Baku subway in the Azerbaijan Republic (1995) and many others [2], there is a continued interest to better understand the fire and smoke behavior in a confined environment such as transit stations and tunnels. Many studies have been done: computational fluid dynamics (CFD) was used to characterize the smoke movement in a subway station and compared with field measurements [3]; the emergency ventilation capacity for an existing rail station was examined using the fire dynamics simulator (FDS) and the results demonstrated that a longer evacuation time could be provided with a higher smoke exhaust rate [4]; Kang (2006) evaluated the effects of smoke blockage, i.e., of station stairways, and showed that it could significantly holdup passengers during evacuation [5].

While CFD has become a proven tool for smoke modeling, the link between the numerical solution and the assessment of the environmental tenability is important and needs to be established. Among all the tenability criteria, such as temperature, radiant heat flux and toxicity, the reduction in visibility due to smoke obscuration has been regarded as the most critical factor [6]. An environment with low visibility would not only mean a much slower walking speed [8], but also could incur psychological or hazardous consequences due to excessive heat exposure, intoxication or fall injuries [7, 8]. As the primary means of smoke control for underground transit stations is by ventilation, the smoke spread and hence tenability would be better understood by examining the visibility conditions. An appropriate method to evaluate visibility for CFD is therefore, necessary.

Jin presented a number of models to predict visibility due to fire smoke [7], and the recent study [9] has included in their mathematical correlation the effects of smoke adherence on exit signs. The most widely used visibility model, especially for CFD, is probably Jin's correlation [10], which states that the product of visibility, V, and the smoke extinction coefficient, C_s, is a constant, that is, $V \times C_s = K$, where K is a constant and takes on different values for light emitting ($K = 5 \sim 10$) or reflecting signs ($K = 2 \sim 4$) [7, 10]. The same formula has been implemented in the fire dynamic simulator (FDS) [11].

However, it should be noted that this correlation would not be applicable because 1) visibility is directional dependent, i.e., based on line of sight, and 2) the smoke distribution is inhomogeneous.

In this study, the visibility is calculated as a line integral along the line of sight through the inhomogeneous smoke layers. This way, other factors such as lighting, shadows and background contrast [7] is excluded. The calculated visibility was referred to as light transmission [12], attenuation or smoke obscuration. The line integration is implemented using a simplified ray-tracing model [13], which is first presented in this paper, and the application of this model is then demonstrated for a mid-platform train fire in an underground rail station. Both natural ventilation and a concept of mechanical ventilation are evaluated, and the visibility conditions are compared at three selected locations along the egress paths. The egress accessibility during emergency evacuation and further developments of the smoke visibility model are also discussed.

METHOD

Smoke Visibility

Bouguer's law is the basis for optical measurements of smoke [14]. It relates the incident light intensity I_0, with the exiting intensity I, after a travel distance S (Eq. [1]). Because the extinction coefficient is a variable and depends on the spatial distribution of smoke concentration, Eq. [1] is re-written in integral form, using a differential path length ds, and integrating along the line of sight, as shown below in Eq. [2],

$$I/I_0 = \exp(-\alpha S) \quad [1]$$

$$I/I_0 = \exp(-\int_S \alpha(s)ds) \quad [2]$$

Where the light extinction coefficient α, equals the product of the mass specific extinction coefficient α_m, and the concentration of smoke m_s, that is,

$$\alpha = \alpha_m m_s \quad [3]$$

In discretized form, Eq. [2] is,

$$I/I_0 = \exp(-\sum_i \alpha_i s_i) \quad [4]$$

Assuming that the integration step size, $s_i = s$, is a constant, and the mass specific extinction coefficient, α_m is a constant [14], substitute Eq. [3] into Eq. [4], gives,

$$I/I_0 = \exp(-s\sum_i \alpha_m \rho_i \omega_{s,i}) = \exp(-s\alpha_m \sum_i \rho_i \omega_{s,i}) \quad [5]$$

Eq. [5] requires input of the mixture density ρ_i, and the mass concentration of smoke $\omega_{s,i}$. This is needed at each integration step along the line of sight. Both the mixture density and the smoke mass fraction can be obtained from the CFD solutions.

By definition, the smoke visibility is the distance traveled before the ray's intensity drops too low to be discernible, i.e., below a threshold value I_t, that is,

$$I = I_0 \exp(-s\alpha_m \sum_{i=1}^{n} \rho_i \omega_{s,i}) \le I_t \quad [6]$$

Because the threshold light intensity would be subjective to one's perception, a graphical approach is used here by relating the reduction in light intensity, I/I_0, directly to smoke obscuration, i.e., opacity = $(1 - I/I_0)$. Since both the reduction in light intensity, I/I_0, and the opacity vary from zero to one, no adjustment is needed for the graphical approach. The visibility distance can then be estimated by referencing the geometric objects in the rendered image.

Numerical Implementation

The smoke model includes a ray-tracing algorithm and other developments such as the interfaces with the numerical data and computer visualization. Essentially the ray-tracing algorithm computes a cluster of rays that shoot from a single point and projects the ray-integral properties to each pixel within the view port [15]. Each ray can be terminated at a wall surface or by any arbitrary bounding volume. The steps of ray-tracing are as follows:

- Set up camera location and orientation.
- Set up view port and its resolution.
- For each ray from the camera through each pixel center on the view port,
    - Compute along the ray,
        - The mixture density, and
        - The mass fraction of smoke.
    - Composite transparency / opacity.
    - Continue until ray terminates.
- Set the opacity of the pixel and assign its color values (Eq. [5]).

It should be noted that ray tracing is used to obtain a *quantitative measure* of smoke visibility rather than the visual effects. A few measures are implemented to reduce the computational cost. The first one is the use of a constant integration step size. For the mesh in general, the geometric aspect ratio of polyhedral control volumes should be close to unity, and there should not be any abrupt jump in mesh sizes. A constant integration step is thus feasible. The second measure is that the numerical interpolation uses the nearest cell-center data, the so-called "nearest point average". This is fast and avoids the time-consuming ray-object intersection tests. Although there are higher order interpolation schemes like tri-cubic spline, the nearest point average is applicable regardless of the control volume types, particularly for a hybrid mesh scheme. The computational time can be further reduced using a pre-defined bounding volume (i.e., box), so only a sub-domain is used instead of the entire computational domain. Finally, for a fixed camera location and orientation, an index table can be set up in advance to identify the control volume indices that each ray passes. Subsequent calculations are simply data extractions and can be done in real-time.

Further details of ray tracing and the smoke visibility model can be found in an earlier study on compartment fire [13]. The model separates the "volume" data from other geometric objects, such as walls and windows, which are processed separately as surface-based graphics. Effectively, smoke visibility acts as a mask to the "clear" scene with no smoke. The composed image is in RGBA format, and the smoke obscuration is obtained by controlling each pixel's opacity through each pixel's alpha channel. The capability of modeling local lighting sources is currently being developed.

DESCRIPTION OF STATION

Station Configuration

The station considered here has a center platform, and has two levels below grade. This station is previously studied for thermal comfort [16] using the Fluent® program [17]. As shown in Fig. 1a, the station cross section has the northbound and the southbound tracks on each side of the platform. The model includes the entire station and two trains. Each train has ten cars, and each car is about 50 ft (15 m) long. The platform is 14 ft (4.3 m) wide and is approximately 550 ft (168 m) long. The ceiling height is 10 ft 8 in (3.3 m) on the platform and 8 ft (2.4 m) on the mezzanine. There are eight stairs along the platform centerline, numbered from south to north as P1 to P8. The stairs are spaced from 30 ft (9.1 m) to 75 ft (23 m) apart. The columns are every 15 ft (4.6 m) along the platform and to the left of the stairs (Fig. 1a). From the mezzanine to the street, there are four stairways, S1-S4, spaced about evenly along the east side. An isometric view of the station is shown in Fig. 1b.

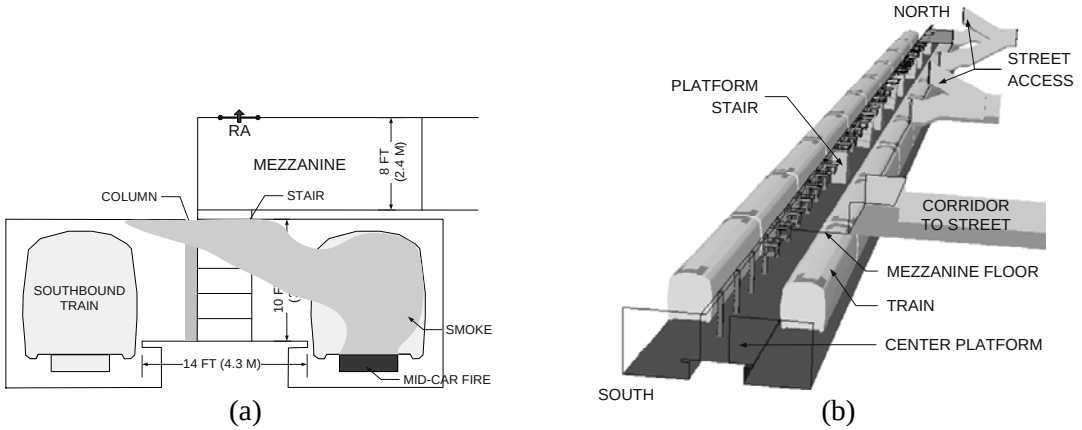

FIGURE 1. Station model, dimensions and fire location

Fire Scenario

As shown in Fig. 2, a t-squared fire of medium growth rate is used to represent the rail car fire. The growth coefficient is $\alpha = 12$ W/s^2. An assumed 120 s lapse time represents a significant ignition source to sustain the fire development. In Fig. 2, the fire heat release rate (HRR) is given by $Q = \alpha\,(t + 120)^2$. The fuel is assumed to be polystyrene with a heat of combustion 39.2 MJ/kg and a smoke yield rate, $Y_s = 0.164$ g/g-fuel [6]. The reaction follows Eq. [7]. The specific extinction coefficient is $\alpha_m = 10$ m^2/g, which is based on the measurements by Mulholland and Croarkin [14].

$$C_8H_8 + 7.42\,(O_2 + 3.76\,N_2) \rightarrow$$
$$5.51\,CO_2 + 3.59\,H_2O + 0.09\,C_8H_8 + 0.22\,CO + 0.11\,CH + 1.42\,C(s) + 27.9\,N_2 \qquad [7]$$

The fire is modeled in CFD using the so-called volumetric heat and mass source (VHMS) method [13]. This approach only considers the heat and mass transfer from the fire in source terms in the conservation equations, but does not simulate the actual combustion. Fig. 3a depicts a possibly "worst-case" fire scenario, in which the fire is on the fifth car of the northbound train and is close to the center of the station. The fire source is located below the car floor as shown in Fig. 1a. As the incident car is close to the four platform stairs, P2, P3, P4 and P5, the smoke from the fire could simultaneously affect these four stairs and the two stairways, S2 and S3 on the mezzanine.

Emergency Ventilation

Both natural ventilation and mechanical ventilation are considered for smoke control. For mechanical ventilation, it could use either the ceiling smoke exhaust at the mezzanine or the tunnel ventilation system. The mezzanine smoke exhaust, as indicated by the line segment marked as "RA" (return air) in Fig. 1a, has a maximum rate of 350 kcfm (165 m^3/s) linearly along the ceiling. As this might not be sufficient, a tunnel ventilation system can be used to exhaust the smoke from both end of the station platform. This is the so-called "all-exhaust" mode of ventilation. The exhaust capacity at each end of the station is 350 kcfm (165 m^3/s).

These ventilation rates are implemented in the CFD model as time-dependent velocity boundary conditions. The smoke spread under both natural ventilation and mechanical ventilation are evaluated separately. Under the mechanical ventilation, the mezzanine smoke exhaust is started first at 30 s after the fire. At 4 min, the mezzanine exhaust is switched off when the all-exhaust mode is activated. A 30 s linear transition to reach full capacity is assumed (Fig. 2). Note that this timeline is based on the continuous monitoring of the smoke dispersion.

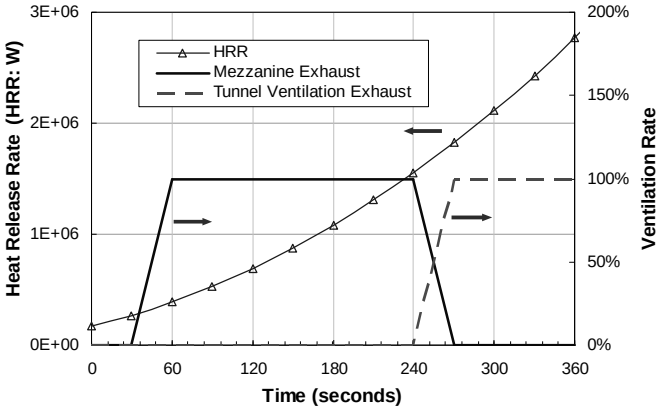

FIGURE 2. Description of the fire curve and the emergency ventilation timeline

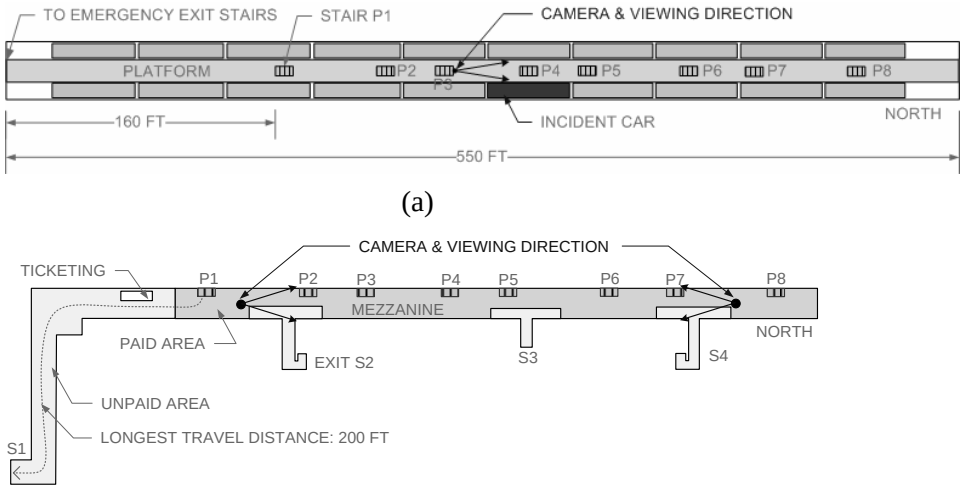

FIGURE 3. Station platform and mezzanine plan, fire car location and the three locations of camera and viewing direction

Model Setup

Three locations are selected from the anticipated escape routes. These locations are marked in Fig. 3 as camera and viewing directions. On the platform, it is at the entrance to stair P3 and is 5 ft (1.5 m) from the floor. The camera is pointing towards stair P4 and the incident car is on the right. The field of view (FOV) angle is about 60°, which is the typical viewing angle of human being [13]. This location is selected to examine the visibility conditions between stairs P3 and P4. A bounding volume, defined by the platform public area between P3 and P4, is used to reduce the computational cost of ray tracing. This location is expected to be the worst on the platform due to its proximity to the fire car.

On the mezzanine, one camera is located at the south end between stair P1 and P2; and the other is on the north between stair P7 and P8. Both are 3.6 ft (1.1 m) above the floor, pointing towards the center as shown in Fig. 3. Because the smoke could block station exits S2 and S3, the only viable escape routes would be from P1 to S1 at the south end and from P7 / P8 to S4 at the north end. From these two locations, it is expected that the visibility conditions will determine how long these egress paths can be kept clear of smoke, or how soon the egress through S2 and S3 are affected.

RESULTS

Platform

Fig. 4a shows the camera view port on the platform, in which the geometrical objects such as the platform, stair P4 and the trains are marked. These objects can be used as references and are drawn as lines or wire frames. The distance between the camera and the entrance to stair P4 is about 10 m.

The reduction in visibility during the first 4 min is shown in Fig. 4. The smoke stratification can be clearly seen within the first minute. Despite smoke spillage to the mezzanine from the stair P4 opening, the visibility indicates smoke layer height drops to about 50% of the ceiling height at 30 s (Fig. 4b). From 30 s to 60 s, the smoke exhaust at the mezzanine starts, and the clearance height remains at about 50% of the ceiling height. After 60 s, the ventilation rate at the mezzanine stays constant (Fig. 2b) and the smoke layer starts to descend towards the platform floor. From 120 s to 150 s, the visibility conditions are similar. Stair P4 is only partially visible, which gives a visibility distance about 10 m near the floor (Fig. 4e). At 150 s, the visibility of stair P4 is nearly lost. This gets worse quickly from 150 s to 180 s. At 180 s, only the nearest floor area is visible, indicating an almost zero visibility. The view port at 240 s shows that the platform area is almost completely blocked by smoke (Fig. 4h).

As the linear grayscale represents smoke obscuration, quantitative obscuration percentages can be obtained by sampling selected viewing directions. This is used to quantify the visibility conditions. Fig. 4c shows the four sampling locations on the centerline of the view port, in which the first point is at the center of the view port, and the second and the third point is at “top” and “bottom”, that is, 75% and 25% of the view port height, respectively. Note that these three points represent three lines of sight, i.e., looking straight ahead, up and down. The location of the fourth point is not fixed but is used to mark the location of 90% obscuration on the centerline. This is to quantify the smoke layer and clearance height.

In Fig. 5, the variation of smoke obscuration is evaluated as a function of time for both natural and mechanical ventilation. Both curves are under natural ventilation during the first 30 s and so they are the same. The effect of mezzanine smoke exhaust can be clearly seen in Fig. 5a. At 60 s, the smoke obscuration is about 50% at the center point and about 20% at the bottom point, whereas under natural ventilation, they are nearly 90% and more than 40%, respectively. At the top point, the condition is similar between the two cases, reaching 90% at 30 s and 100% at 60 s. After 60 s, as the

smoke exhaust rate levels off, it can be seen that the situation on the platform gets worse quickly (Fig. 5a). The obscuration at the center point reaches 90% at about 120 s and the bottom is at about 240 s. If using the 90% obscuration as a threshold, the condition at the center point is much better with the mezzanine smoke exhaust. However, beyond 150 s, the smoke obscuration at the bottom point is slightly worse than the natural ventilation case.

Using 90% obscuration on the centerline, the smoke layer height is evaluated from the position of the fourth sampling point (Fig. 4c). This is shown in Fig. 6 for both natural and mechanical ventilation. With the mezzanine smoke exhaust, the smoke layer is first kept at 6 ft (1.82 m) or 40% of the ceiling height till 60 s, and then drops to 5 ft (1.52 m) or 50% until 150 s. From 150 s, the smoke layer starts to descend. The two curves converge at about 180 s indicating that the mechanical ventilation cannot control the smoke at this time. The sudden drop of the smoke layer height at 240 s is expected from the "all-exhaust" tunnel ventilation.

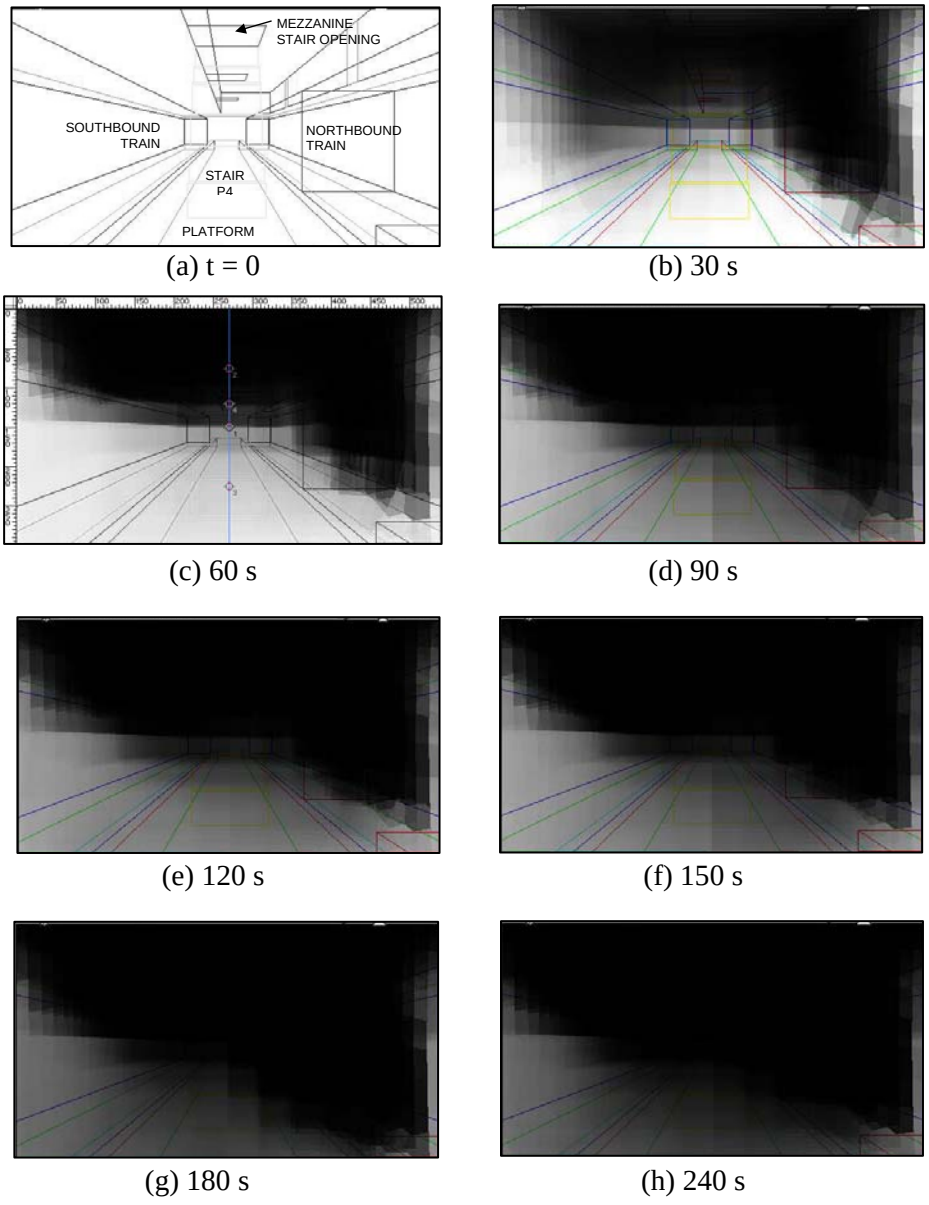

FIGURE 4. Smoke obscuration on the platform during the initial 4 min with mechanical ventilation

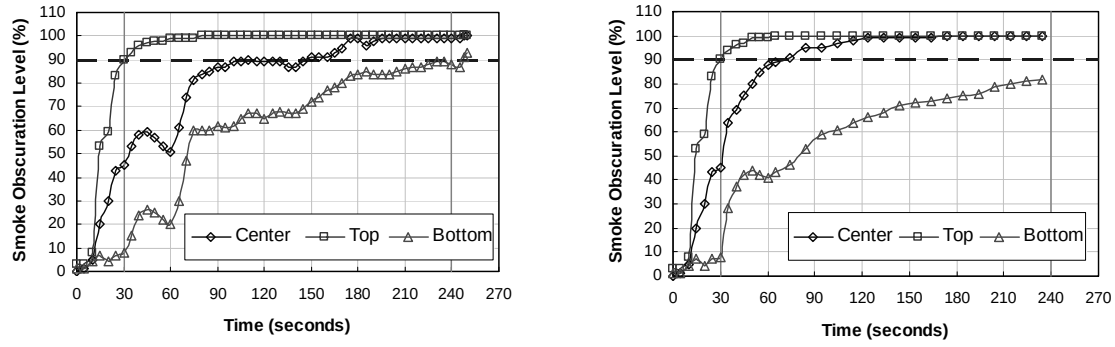

(a) (b)

FIGURE 5. Variation of smoke obscuration as a function of time on the platform with (a) mechanical ventilation and (b) natural ventilation; Dash line is 90% obscuration

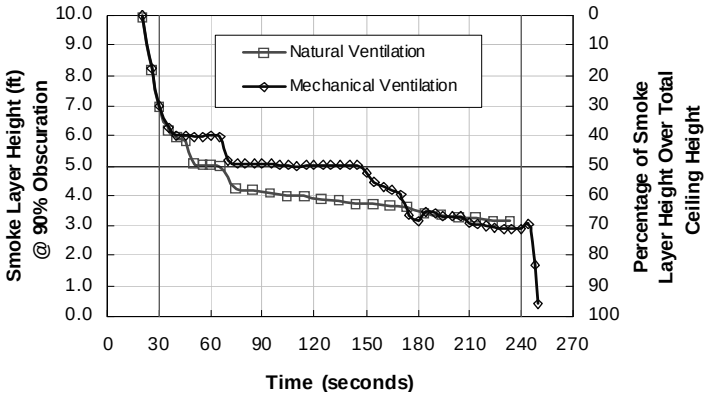

FIGURE 6. Estimated smoke layer height on the platform using 90% obscuration level under natural and mechanical ventilation

Mezzanine

As the smoke spreads underneath the ceiling on the platform, the spillage of the smoke through the stairway openings causes reduction in visibility on the mezzanine. At 240 s, Fig. 7a shows that exit S2 is only partially visible and is about 50% blocked. The mezzanine seems to have filled with smoke. The visibility distance near the floor is less than 10 m. At 270 s, the smoke is pulled back towards stair P4 (Fig. 7b) due to the tunnel smoke exhaust (Fig. 2b). The make-up air from the street exits dilutes the smoke and improves the visibility condition on the mezzanine. Fig. 7b shows that the visibility near the floor is about 30 m on the left, but remains about 10 m on the right near exit S2. This can be explained by the flow pattern: as the make-up air flows down from exit S2, the sudden expansion as it enters the mezzanine forms a re-circulation zone near the right sidewall. The smoke residual is due to this re-circulation zone.

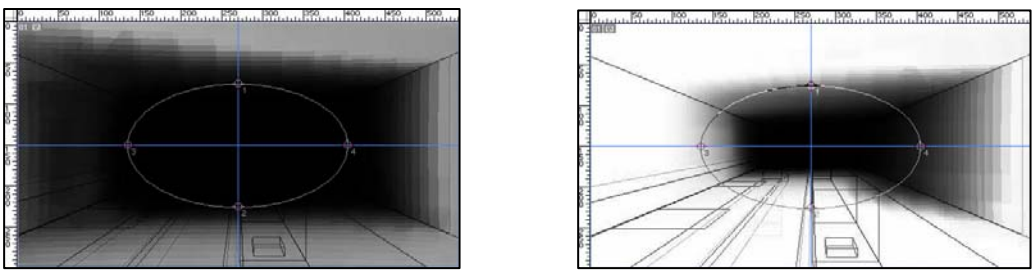

(a) t = 240 s (b) t = 270 s

FIGURE 7. Smoke obscuration at the south end of the mezzanine

Using the same approach as for the platform, five sample points are selected representing typical viewing directions. The first four points (Fig. 7) are referred to as the "top", "bottom", "left" and "right" points, respectively. An elliptic circle is used to control the relative position of these four points. The "center" point is at the intersection of the two centerlines in the view port. Fig. 8 shows the variation of smoke obscuration levels under natural and mechanical ventilation. Under natural ventilation, the smoke obscuration levels at all the points except the center are affected almost simultaneously at 45 s (Fig. 8a). Within t = 90 s, the smoke obscuration levels exceed the 90% threshold at all locations. While under mechanical ventilation, the breach of the 90% threshold is delayed to about t = 210 s (Fig. 8b); and from t = 240 s, the tunnel ventilation clears the smoke out of the mezzanine within about 60 s. Note that the offset from zero for the "bottom" point is because of the overlapping line object in the background.

Because the camera at the north end is further away from the fire than that at the south (Fig. 3b), the visibility condition at the north end is much improved (Fig. 9). Note that the variations of smoke obscuration at the center point are almost the same between the two camera locations. This is as expected and shows good consistency of the ray integration, i.e., reciprocity. It should also be noted that the rate of increase in smoke obscuration is high, less than 30 to 60 s (Fig. 5, Figs. 8 and 9), suggesting the rapid loss of visibility for such fire.

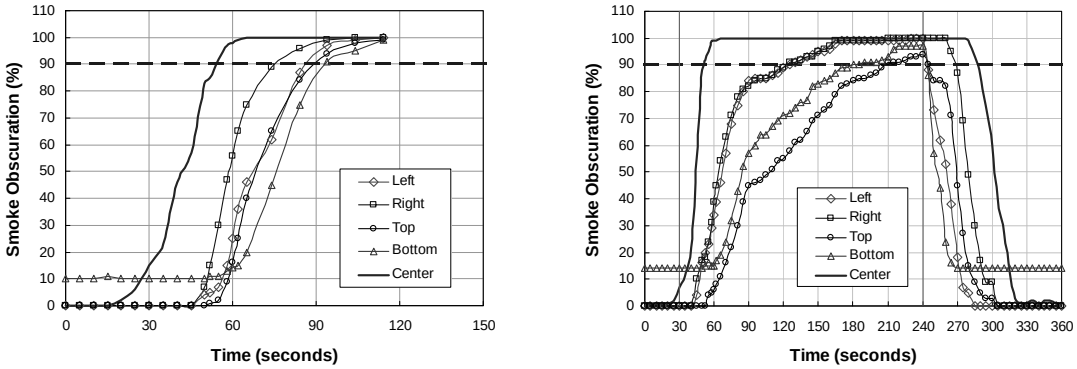

FIGURE 8. Variation of smoke obscuration levels as a function of time at selected viewing directions at the south end of the mezzanine: (a) natural ventilation, and (b) mechanical ventilation; Dash line is 90% obscuration

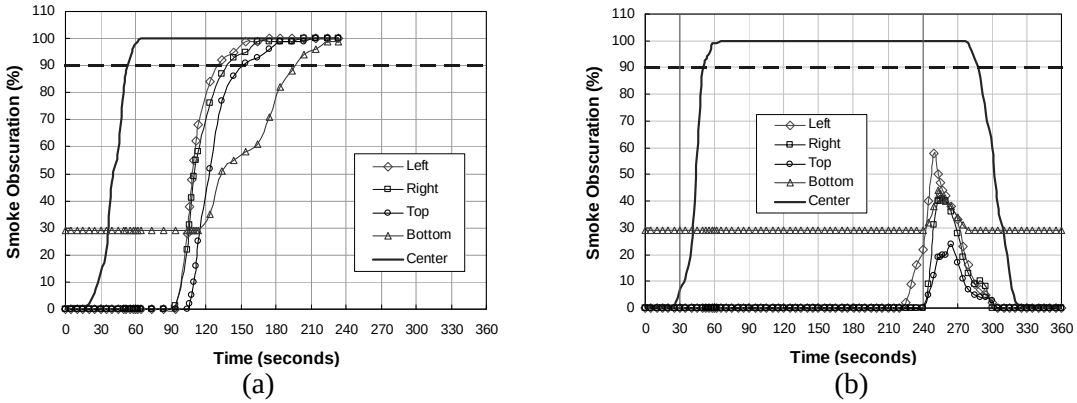

FIGURE 9. Variation of smoke obscuration levels as a function of time at selected viewing directions at the north end of the mezzanine: (a) natural ventilation, and (b) mechanical ventilation; Dash line is 90% obscuration

DISCUSSION

The predicted smoke obscuration can be related to tenability, and this should be useful in determining the tenable time available for egress, such as the accessibility of stairways. While other factors are mostly consequential due to over-exposure to fire and / or smoke, such as incapacitation, it should be noted that smoke visibility might be more suitable in determining the egress accessibility, for example, when visibility reduces to below 30 ft (10 m), statistical data have shown that 97% of the British and 94% of the US populations initiated the "turned back" behavior [8]. In a related study [5], it was assumed that a 20%-smoke-obscuration over a 10-ft (3-m) long stairway opening would cause sufficient concern that people tend to avoid during evacuation. This is equivalent to a visibility distance of approximately 50 ft (15 m). Using this criterion, the times of accessibility of the stairways are estimated (TABLE 1). A much longer required-evacuation-time is demonstrated taking into account the stairway accessibility [5].

TABLE 1. Predicted time of accessibility of the stairways under mechanical ventilation [5]

Location	**Time of Accessibility* for Stairway and Exits (seconds)**							
Platform	P1	P2	P3	P4	P5	P6	P7	P8
	>240	80	31	14	33	160	>240	-†
Mezzanine	S1	S2		S3		S4		
	-†	n/a‡		n/a‡		-†		

*"Time of Accessibility" estimated based on 20% smoke obscuration on the mezzanine;
†Not affected by smoke; and
‡Not applicable, as the make-up air keeps the stairways clear of smoke.

Conversely, the results of the smoke obscuration can be related to optical smoke detector and video images. A number of field tests on smoke detection in tunnels have suggested a similar approach by tracking the image contrast levels [18, 19]. The prediction of smoke obscuration has not considered lighting, especially discrete light source, instead, the initial light intensity is assumed uniform. Note that in reality, the smoke layer blocks the ceiling light sources and the shadow further reduces the visibility near the floor, the visibility conditions shown here may be the "maximum" or "optimum" visibility. The effect of lighting on visibility is being developed, and it is expected that, with further improvement, this model would not only be useful in the development of efficient algorithms for smoke detection, but also for the positioning of video cameras.

The smoke visibility model allows for evaluation of visibility based on line of sight. Previous studies have either used the light extinction coefficient or the spatial distribution of "local visibility". The latter comes from the experimental correlation (Jin [7, 10]), $V = K / C_s$. The deficiency of these methods has been shown for a compartment fire [13], suggesting the difficulty in selecting a threshold smoke concentration to represent visibility, and that using the spatial smoke distribution could be misleading in tenability assessment. This is illustrated using the smoke obscuration in Fig. 4and the distribution of smoke mass fraction in Fig. 10. First, note that the two Figures paint a different picture in terms of tenability. From t = 180 s to 240 s, Fig. 10 shows significant increase of smoke on the mezzanine, whereas the smoke layer near the platform ceiling remains stratified and only deepens slightly; in contrast, examination of the smoke obscuration suggests that the visibility near the floor is almost lost between 180 s and 240 s (Fig. 4), rendering the entire section untenable. The predicted smoke obscuration is qualitatively consistent with Jin's correlation, for example, a mass fraction of 2×10^{-5} for a 10-m visibility can be obtained using C = 2.0 for stairways in underground arcades [10]. The smoke layer of this concentration does shift slightly deeper near stairway P3 at t = 240 s (Fig. 10), which supports the visibility predictions. However, it should be noted that visibility is the distance along the line of sight and the associated three-dimensionality is difficult to assess from the two-dimensional (2D) contours of smoke distribution. Finally, this comparison indicates that any meaningful 2D presentation of smoke distribution should be scaled and examined in

such a way that the entire anticipated visibility range can be captured, that is, the lower bounds of smoke concentration should be represented.

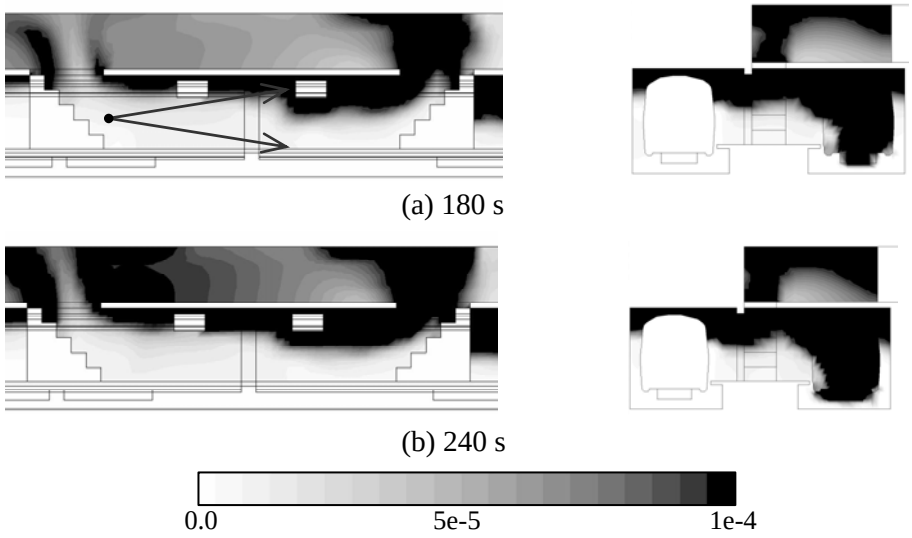

FIGURE 10. Distribution of smoke mass fraction in the longitudinal mid-plane and transverse section of the station under mechanical ventilation; linear grayscale of smoke mass fraction is from zero to 10^{-4} kg-smoke/kg-mixture

A number of observations can be made on the smoke propagation and the visibility predictions. First, the results show that during a train fire, visibility in the station could reduce to zero or only a few meters within one to two minutes. This is consistent with the records of underground station and tunnel fires [1], and suggests that effective smoke management is crucial to station fire safety, which includes emergency ventilation as well as other measures such as fire and smoke detection, egress, system control and emergency response. Second, the results (TABLE 1) show that the platform stairways could be smoke-logged in a short time and become inaccessible for passenger evacuation and fire rescue. Being able to use emergency exit stairs is, therefore, critical for a timely and safe evacuation in case of inevitable loss of stairways due to fire smoke [5]. Third, since visibility is generally regarded as the most critical factor [6], the smoke visibility model allows for detailed examination of environmental tenability, for example, the smoke layer height in Fig. 6 is evaluated from the camera 5 ft (1.5 m) above the floor and is based on view projection. This is from the passenger's perspective and is likely to be different from the "height of the first indication of smoke" [20] that is based on smoke concentration. The US railway standard NFPA 130 [21] prescribes visibility as one of the tenability criteria, the smoke visibility model is to try to answer to that requirement, for example, the quantitative assessment in Fig. 4. However, it should be noted that the parameters used in the visibility calculation, especially the mass specific extinction coefficient, would need further experimental verification.

CONCLUSIONS

In this paper, a smoke visibility model is presented for CFD application in smoke control. A simplified ray-tracing technique is developed to calculate smoke obscuration as line integrals. Using this model, the visibility condition in a rail station is examined under a design fire scenario of mid-platform train fire. The model setup emulates three cameras located at the station egress paths. The results show that the visibility distance could reduce to zero or only a few meters in a short time. Quantitatively, the model compares the performance of natural and the mechanical ventilation and

shows that the designed mechanical ventilation could not contain the smoke in 2 to 3 minutes. The variation of smoke obscuration on the mezzanine is presented, and shows the dependence of visibility on view direction and demonstrates the reciprocity of the line integration. Using smoke distribution in the mid-plane of the platform, the comparison shows that the predicted smoke obscuration agrees qualitatively with the experimental correlation, and that the three-dimensionality associated with visibility is difficult to assess from two-dimensional contours of smoke distribution. The predicted smoke visibility would be useful in egress accessibility assessments and the potential application to smoke detection such as detection algorithms and the positioning of video cameras. Further developments of the model would include discrete lighting effects and model validation.

REFERENCES

1. Chien, S-W., Chen, W-L., Shen, T-S., Cheng, C-C., Lee, D-C., Hsuse, Y-L. and Chen, T-K., "A Study on the People Evacuation Safety for the Underground MRT Station", Proceedings of the 6th Asia-Oceania Symposium on Fire Science and Technology, March 17-20, 2004, Daegu, Korea, 2004.
2. Carvel, R. and Marlair, G., "A History of Fire Incidents in Tunnels", in Handbook of Tunnel Fire Safety, ed. A. Beard and R. Carvel, Thomas Telford Publishing, 2005.
3. Moriyama, S., Hasemi, Y., Nam, D., Tanaka, S., Okazawa, N. and Ding, W., "Smoke Movement Characteristics and Fire Safety in Subway Stations", Proceedings of the 8th Intl Symp for Fire Safety Science, Beijing, China, pp. 1461-1470, Sept 2005.
4. Park, W.H., Kim, D.H. and Chang, H.C., "Numerical Predictions of Smoke Movement in a Subway Station under Ventilation", Tunnelling and Underground Space Tech, 21: 3-4, 304, May-July 2006.
5. Kang, K., "Application of NFPA-130 to Emergency Evacuation in a Mass Transit Station," ASHRAE Transactions, 112: Part 2, 266-274, 2006.
6. Klote, J.H. and Milke, J.A., Principles of Smoke Management, American Society of Heating, Refrigerating, and Air-Conditioning Engineers (ASHRAE) and Society of Fire Protection Engineers (SFPE), Quincy, MA, 1997.
7. Jin, T., "Section 2, Fire Dynamics, Chapter 4: Visibility and Human Behavior in Fire Smoke", in The SFPE Handbook of Fire Protection Engineering, ed. DiNenno, P.J. et al., 3rd ed., Society of Fire Protection Engineers (SFPE) and National Fire Protection Association (NFPA), Quincy, MA, 2002.
8. Bryan, J.L., "Section 3, Hazard Calculations, Chapter 12: Behavioral Response to Fire and Smoke", in The SFPE Handbook of Fire Protection Engineering, ed. DiNenno, P.J. et al., 3rd ed., Society of Fire Protection Engineers (SFPE) and National Fire Protection Association (NFPA), Quincy, MA, 2002.
9. Akizuki, Y., Tanaka T., Suzuki, H. and Tsuchihashi, T., "Calculation Method for Visibility of Emergency Sign in Fire Taking into Account of Smoke Adherence", Proceedings of the 8th Intl Symp for Fire Safety Science, Beijing, China, pp. 1093-1102, Sept 2005.
10. Jin, T. and Yamada, T., "Irritating Effects of Fire Smoke on Visibility", Fire Science and Technology, 5: 1, 79-90, 1985.
11. McGrattan, K.B. and Forney, G.P., Fire Dynamics Simulator (version 4) – User's Guide, p. 57, National Institute of Standards and Technology (NIST), SP1019, Gaithersburg, MD, 2006.
12. US DOT / FAA, Computational Fluid Dynamics Code for Smoke Transport during an Aircraft Cargo Compartment Fire: Transport Solver, Graphical User Interface, and Preliminary Baseline Validation, p. 31, Office of Aviation Research, Washington, DC, 2003.
13. Kang, K., "Modeling Smoke Visibility in CFD," Proceedings of the 8th Intl Symp for Fire Safety Science, Beijing, China, pp. 1265-1276, Sept 2005.
14. Mulholland, G.W. and Croarkin, C., "Specific Extinction Coefficient of Flame Generated Smoke", Fire Mater, 24:227-230, 2000.
15. Foley, J., van Dam, A., Feiner, S. and Hughes, J., Computer Graphics Principles and Practices, Addison Wesley, 1990.

16. Kang, K., “Analysis of Platform Spot Cooling in an Underground Subway Station”, Intl J of Ventilation, 3: 3, 235-244, 2004.
17. Fluent, Inc., Fluent v6.1 User’s Guide, Lebanon, NH, 2003.
18. Ono, T., Ishii, H., Kawamura, K., Miura, H., Momma, E., Fujisawa, T. and Hozumi, J., “Application of Neural Network to Analyses of CCD Colour TV-Camera Image for the Detection of Car Fires in Expressway Tunnels”, Fire Safety J, 41:4, 279-284, 2006.
19. Versavel, J. and Roelants, I., “Improving Road and Tunnel Safety via Incident Management: Implementing a Video Image Processing System”, The 2nd Intl Symp of Safe & Reliable Tunnels: Innovative European Achievements, Lausanne, Switzerland, 2006.
20. NFPA, NFPA 92B: Standard for Smoke Management Systems in Malls, Atria, and Large Spaces, National Fire Protection Association, Quincy, MA, 2005.
21. NFPA, NFPA 130: Standard for Fixed Guideway Transit and Passenger Rail Systems, National Fire Protection Association, Quincy, MA, 2007.